Journal of Solid State Chemistry 184 (2011) 589–596

Contents lists available at ScienceDirect

Journal of Solid State Chemistry

journal homepage: www.elsevier.com/locate/jssc

Effect of water vapor on the thermal decomposition process of zinc hydroxide chloride and crystal growth of zinc oxide

Takahiro Kozawa [a], Ayumu Onda [a], Kazumichi Yanagisawa [a,*], Akira Kishi [b], Yasuaki Masuda [b]

[a] Research Laboratory of Hydrothermal Chemistry, Faculty of Science, Kochi University, 2-5-1 Akebono-cho, Kochi 780-8520, Japan
[b] Rigaku Corporation, 3-9-12 Matsubara-cho, Akishima-shi, Tokyo 196-8666, Japan

ARTICLE INFO

Article history:
Received 23 July 2010
Received in revised form
6 January 2011
Accepted 16 January 2011
Available online 25 January 2011

Keywords:
Zinc hydroxide chloride
Zinc oxide
Water vapor
Thermal decomposition
Thermal analysis
Crystal growth

ABSTRACT

Thermal decomposition process of zinc hydroxide chloride (ZHC), $Zn_5(OH)_8Cl_2 \cdot H_2O$, prepared by a hydrothermal slow-cooling method has been investigated by simultaneous X-ray diffractometry and differential scanning calorimetry (XRD–DSC) and thermogravimetric-differential thermal analysis (TG-DTA) in a humidity-controlled atmosphere. ZHC was decomposed to ZnO through β-Zn(OH)Cl as the intermediate phase, leaving amorphous hydrated $ZnCl_2$. In humid N_2 with $P_{H_2O}=4.5$ and 10 kPa, the hydrolysis of residual $ZnCl_2$ was accelerated and the theoretical amount of ZnO was obtained at lower temperatures than in dry N_2, whereas significant weight loss was caused by vaporization of residual $ZnCl_2$ in dry N_2. ZnO formed by calcinations in a stagnant air atmosphere had the same morphology of the original ZHC crystals and consisted of the *c*-axis oriented column-like particle arrays. On the other hand, preferred orientation of ZnO was inhibited in the case of calcinations in 100% water vapor. A detailed thermal decomposition process of ZHC and the effect of water vapor on the crystal growth of ZnO are discussed.

1. Introduction

Metal hydroxide salts (MHSs) with layered structures have been widely studied for applications such as ion exchangers, catalysts, biosensors, and drug delivery agents [1–6]. An additional potential application for these solids is the precursor to metal oxides by the thermal decomposition [6]. In some cases, thermal decomposition proceeds with a topotactic process, as in the case of Ni/Al_2O_3 and $Ni/NiAl_2O_4$ composites obtained from Ni/Al layered double hydroxides [7], and of the formation of cobalt oxide [8] and magnesium oxide [9]. Therefore, thermal transformation of varied MHSs compounds is an effective method to yield corresponding oxides with controlled morphologies. In particular, transformation from zinc hydroxide salts (ZHSs) to zinc oxide (ZnO) by the thermal decomposition has got attention, because ZnO is of particular interest in view of its low toxicity and a wide range of possible applications, including transparent conductive electrode, catalyst and photo-catalyst, solar cell technology, and fluorescent substance [10–12].

The thermal decomposition behavior and properties of ZnO obtained from ZHSs strongly depends on the precursors of ZHSs. Morioka et al. [13] reported the production of ZnO powders with film-like morphology by the thermal decomposition of $Zn_5(OH)_8(CH_3COO)_2 \cdot 2H_2O$, and Hosono et al. [14] also prepared porous ZnO films in the same manner. Biswick et al. [15,16] have investigated the thermal decomposition process of $Zn_5(OH)_8(CH_3COO)_2 \cdot 4H_2O$ and $Zn_5(OH)_8(NO_3)_2 \cdot 2H_2O$. A detailed study of the early growth stages of the nanoscale ZnO crystallites obtained from thermal decomposition of four different precursors (hydroxide nitrate, oxalate, hydroxide carbonate, and acetate) has been reported by Audebrand et al. [17]. ZnO sheets with hexagonal plates in shape were obtained by calcination of hexagonal plate-like crystals of zinc hydroxide chloride (ZHC), $Zn_5(OH)_8Cl_2 \cdot H_2O$, obtained by the hydrothermal slow-cooling method [18].

Arii and Kishi [19] have been conducted the thermal decomposition of $Zn(CH_3COO)_2 \cdot 2H_2O$ in some humidity controlled atmospheres by using a novel thermal analyses, which are sample-controlled thermogravimetry (SCTG), thermogravimetry combined with evolved gas analysis using mass spectrometry (TG-MS), and simultaneous measurement of X-ray diffractometry and differential scanning calorimetry (XRD–DSC). The thermal decomposition process of anhydrous zinc acetate was remarkably influenced by the partial pressure of water vapor in the atmosphere [19], and anhydrous zinc acetate was directly decomposed to crystalline ZnO by reacting with the water vapor in a high humidity atmosphere.

The thermal decomposition process of ZHC has been reported by Garcia-Martinez et al. [20] and other researchers [21,22]. Garcia-Martinez et al. [20] investigated the thermal decomposition

* Corresponding author. Fax: +81 88 844 8362.
E-mail address: yanagi@kochi-u.ac.jp (K. Yanagisawa).

0022-4596/$ - see front matter © 2011 Elsevier Inc. All rights reserved.
doi:10.1016/j.jssc.2011.01.015

process of ZHC in terms of a heating rate. As shown by Arii and Kishi [19], the presence of water vapor in the atmosphere may also affect the thermal decomposition process of ZHC. In the present research, we investigated the effect of water vapor on the thermal decomposition process of ZHC to prepare ZnO by using XRD–DSC and TG-DTA equipped with a humidity generator.

2. Experimental section

2.1. Material preparation

Zinc hydroxide chloride (ZHC; $Zn_5(OH)_8Cl_2 \cdot H_2O$) was prepared by the hydrothermal slow-cooling method described in a previous study [18]. Zinc chloride ($ZnCl_2$) and sodium hydroxide (NaOH) were purchased from Wako pure chemical industries, Ltd. (Japan) and used without further purification. In a typical synthesis, a mixed solution of 5 mL of 0.4 M NaOH solution and 50 mL of 1 M $ZnCl_2$ solution was heated in a 70 mL Teflon-lined autoclave to 220 °C without agitation. After the temperature was maintained at 220 °C for 2 h, the autoclave was cooled down to room temperature at the rate of 1 °C/min. The white plate-like crystals obtained after the reaction were filtered, washed with distilled water, and dried in an oven at 60 °C.

2.2. Thermal analysis

The thermal analysis of ZHC obtained by the hydrothermal slow-cooling method was investigated by simultaneous measurements of X-ray diffractometry and differential scanning calorimetry (XRD–DSC) and thermogravimetric-differential thermal analysis (TG-DTA) with two heating patterns at three different H_2O partial pressures. One of the heating patterns was a simple heating from room temperature to 520 °C at a heating rate of 5 °C/min (A). The other involved a cyclic process of heating to 230 °C with a rate of 5 °C/min, keeping at 230 °C for 10 min, cooling to 45–55 °C with a rate of 5 °C/min, keeping at 45–55 °C for 3 h, and finally heating to 520 °C with a rate of 5 °C/min (B). The samples were heated in flowing N_2 (XRD–DSC; 200 mL/min, TG-DTA; 250 mL/min) with different H_2O partial pressures which were controlled by a humidity generator RIGAKU/HUM-1 to be (1) dry N_2 without H_2O, (2) humid N_2 including H_2O partial pressure of 4.5 kPa (saturated water vapor at 31 °C, 4.46% H_2O—95.54% N_2), and (3) humid N_2 including H_2O partial pressure of 10 kPa (saturated water vapor at 46 °C, 9.9% H_2O—90.1% N_2).

The XRD–DSC measurement was carried out with a RIGAKU/XRD–DSC II instrument which consists of a diffractometer (RIGAKU/RINT-ULTIMA III) combined with a heat-flux type DSC instrument (based on RIGAKU/Thermo-Plus DSC 8230 modules). The samples were mounted on a square aluminum container (7 mm × 7 mm and 0.2 mm in depth). A line shape Cu$K\alpha$ X-ray source was operated at 40 kV and 50 mA and the patterns were recorded in the range 8–58° in $2\theta/\theta$ scanning mode with a 0.02° step and scanning speed of 30°/min. The temperature difference was about 10 °C per pattern. The TG-DTA measurement was carried out with Rigaku Thermo Plus 8120D systems for a sample (5 mg) in an aluminum crucible.

2.3. Thermal decomposition

In order to clarify the influence of water vapor on the decomposed products, the ZHC plate-like crystals were heated at 300–500 °C for 30 min in air and a water vapor atmosphere by a tubular furnace equipped with a water evaporator. Thermal decomposition in air was performed in stagnant conditions by removing the evaporator. For water vapor atmosphere, distilled water was introduced at a flow rate of 0.5 mL/min into the evaporator without a carrier gas to generate a 100% water vapor atmosphere in the furnace. Flow rate of water vapor was estimated to be 0.63 L/min. The samples mounted on a platinum plate were put on an alumina boat and the boat was inserted into the furnace preheated to a desired temperature.

2.4. Characterization

The room temperature powder XRD data was collected on a Rigaku Ultima IV X-ray diffractometer using Cu$K\alpha$ radiation at 40 kV and 20 mA. The patterns were recorded in the range 10–80° in $2\theta/\theta$ scanning mode with a 0.02° step and scanning speed of 40°/min. The peak positions and relative intensities of the peaks were compared with the data in the Joint Committee for Powder Diffraction Standard (JCPDS) cards. Micrographs of scanning electron microscopy (SEM) were obtained using Hitachi S-530 operating at 25 kV.

3. Results

3.1. Characterization of the synthesized ZHC crystals

Fig. 1 shows the XRD pattern and SEM image of the product obtained by the hydrothermal slow-cooling method. The sample was spread on a nonreflecting sample holder without grinding in

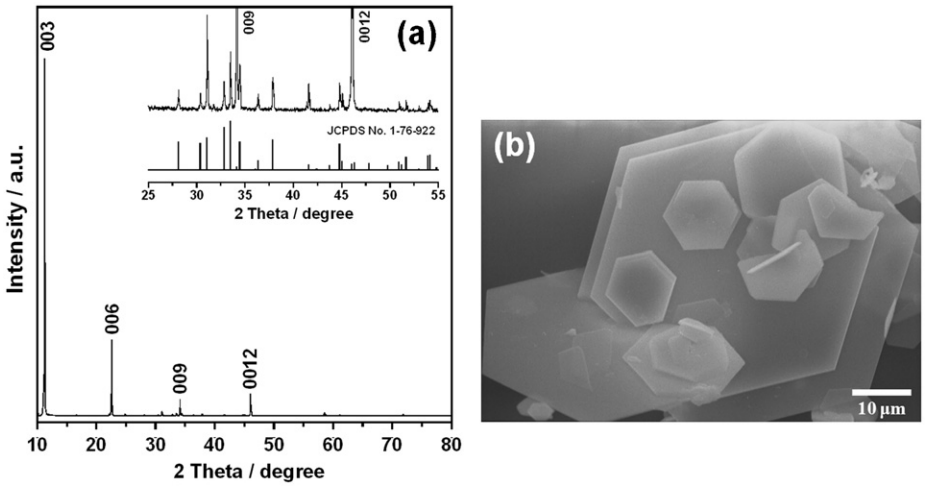

Fig. 1. (a) XRD pattern and (b) SEM image of $Zn_5(OH)_8Cl_2 \cdot H_2O$ (ZHC) obtained by the hydrothermal slow-cooling method. Inset figure in the XRD pattern shows details of the high angle reflections.

such a way that the plate-like crystals were preferred oriented. The product was confirmed to be $Zn_5(OH)_8Cl_2 \cdot H_2O$ (JCPDS no. 1-76-922) and no impurity phases were found as shown in the inset figure of Fig. 1a. The XRD pattern of the product, shown in Fig. 1a, indicates a preferred orientation along the [003] direction. The most intense peak at $2\theta = 11.2^\circ$ (d; 7.88 Å) corresponds to (003) diffraction, the basal plane of the layered structure of ZHC. The peaks at $2\theta = 22.6^\circ$ (d; 3.94 Å), 34.1° (d; 2.63 Å), and 46.0° (d; 1.97 Å) can be assigned to its second, third, and fourth order reflections, respectively. As indicated by the SEM image (Fig. 1b), the ZHC crystals have the hexagonal morphology with lateral size up to 50 μm and thickness of about 1 μm. This morphology gives rise to preferred orientation of the crystals, which causes the characteristic XRD patterns with strong intensities along the [003] direction.

3.2. Thermal analysis

(A) *XRD–DSC measurements*: The ZHC sample was heated to 520 °C in humid N_2 with $P_{H_2O} = 4.5$ kPa at a heating rate of 5 °C/min. Fig. 2 shows the three dimensional plots of the XRD patterns recorded during the heating of ZHC sample (Fig. 2a) and the XRD–DSC plots obtained at a temperature range from 120 to 240 °C (Fig. 2b). Fig. 2a well illustrates that ZHC was decomposed through an intermediate compound to the final product, ZnO. It can be clearly observed that the diffraction peaks of ZnO appears at around 180 °C and the extremely high intensity of the (002) peak at $2\theta = 34.4^\circ$ proves the highly c-axis oriented structure in ZnO particles.

The XRD patterns of the sample at each temperature on the DSC curves are shown in Fig. 2b. The DSC curve showed the

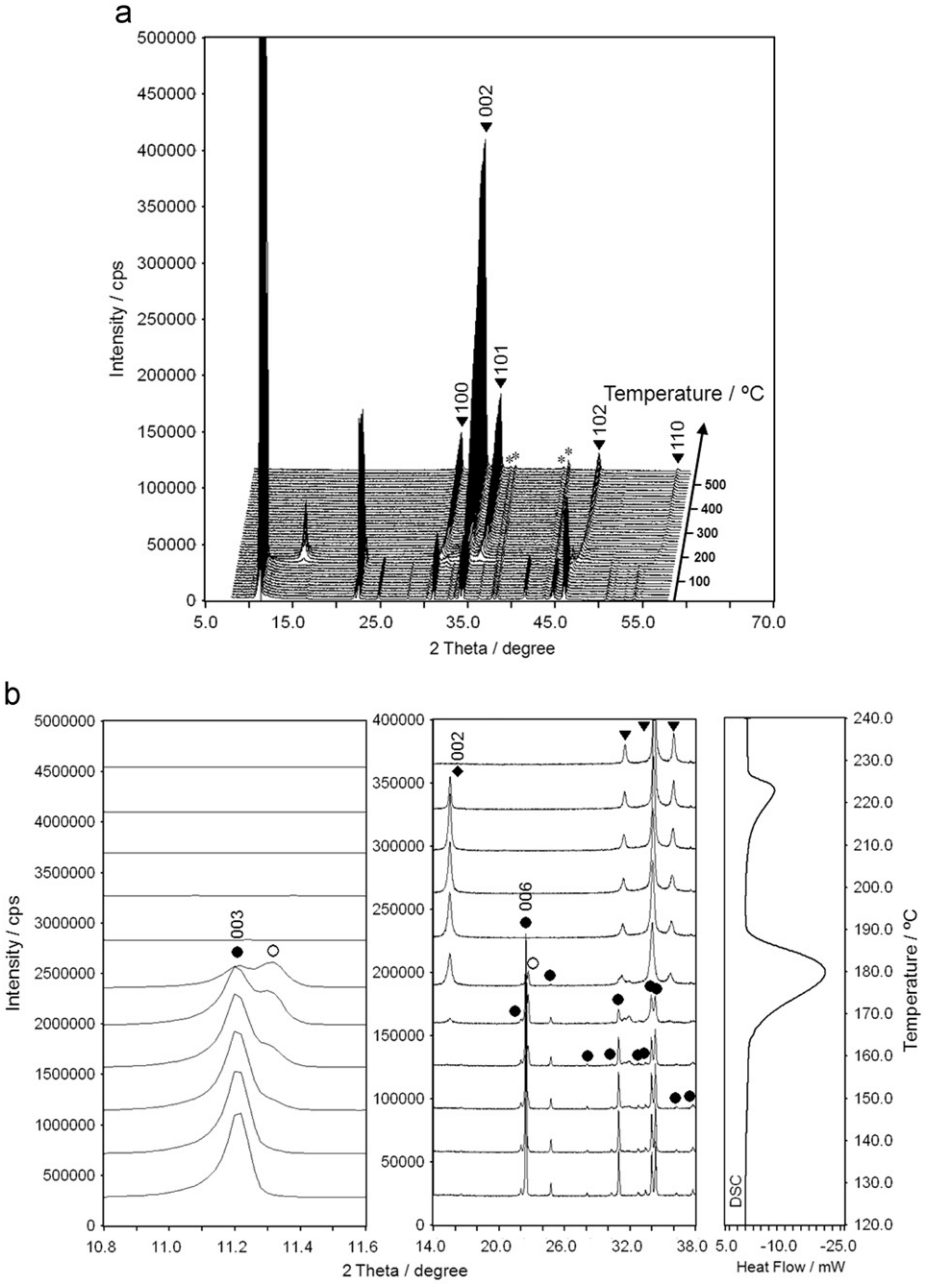

Fig. 2. (a) *In situ* XRD patterns for ZHC-ZnO in humid N_2 with $P_{H_2O} = 4.5$ kPa and (b) relationships between the enlarged XRD patterns (left and middle) and DSC curve (right) recorded from 120 to 240 °C: (●) ZHC, (○) defective structure of ZHC, (♦) β-Zn(OH)Cl, and (▼) ZnO. The each reflection peaks are labeled *hkl* and (*) is a reflection from the sample holder.

two endothermic peaks. The first endothermic peak appeared at temperatures between 160 and 190 °C (T_{max}=180.3 °C). XRD patterns corresponding to this temperature range revealed the decomposition of ZHC, followed by the formation of β-Zn(OH)Cl (JCPDS no. 1-72-525) as the intermediate phase. At the same time, the ZnO phase appeared at around 180 °C. The formation of β-Zn(OH)Cl during the decomposition of ZHC has been reported before [20,21]. It is interesting that β-Zn(OH)Cl with the high intensity of (003) reflection show high *c*-axis orientation. In the temperature range from 160 to 180 °C, the (003) and (006) peaks of ZHC are split and these split peaks marked with "○" correspond to a distance of 7.81 and 3.92 Å, respectively. This splitting can be explained as due to the defective structure of ZHC indicating smaller interlayer spacing being a result of collapsing its layers at higher temperatures. This defective structure of the layered double hydroxide during the thermal decomposition has been observed by some researchers [23,24]. The second endothermic peak appeared between 210 and 230 °C (T_{max}=222.8 °C). This endothermic reaction corresponds to the decomposition of β-Zn(OH)Cl. As indicated by the *in situ* XRD measurements, ZnO was only existed in the product by heating above 230 °C (Fig. 2a).

In dry N_2, two endothermic peaks on DSC curve appeared between 160 and 190 °C (T_{max}=179.5 °C) and between 200 and 225 °C (T_{max}=218.4 °C). Thus, by comparing with the XRD–DSC results obtained in humid N_2, the remarkable differences were not seen in dry N_2.

(B) *TG-DTA measurements*: In order to clarify the influence of water vapor on the ZHC decomposition, TG-DTA was conducted in dry N_2 and humid N_2 with H_2O partial pressure of 4.5 and 10 kPa. The TG-DTA profiles are shown in Fig. 3 with the TG curve obtained in stagnant air. The DTA curve in dry N_2 represents two endothermic peaks at 170 and 451 °C, which correspond to the two weight loss stages. On the other hand, the curves obtained in humid N_2 represent three endothermic peaks with three corresponding weight loss stages at 175, 216, and 387 °C for P_{H_2O}=4.5 kPa, and at 183, 228, and 373 °C for P_{H_2O}=10 kPa, respectively. With the increase in H_2O partial pressure, two endothermic peaks up to 230 °C were shifted to higher temperatures, whereas the other at high temperatures beyond 350 °C was shifted to lower temperatures. On the basis of the XRD–DSC results (Fig. 2b), the first and second weight loss stages in humid N_2 correspond to the dehydration process of the decomposition of ZHC and β-Zn(OH)Cl, respectively. In dry N_2, these two dehydration processes had overlapped at 170 °C.

The amounts of weight loss by heating to 230 °C were same in the range 14.5–15.5% for the four atmospheres (dry, air, P_{H_2O}=4.5 and 10 kPa). According to the results of *in situ* XRD measurements (Fig. 2a), ZnO was only crystalline phase existed in the product by heating at high temperatures beyond 230 °C. However, TG curves showed that the weight loss occurred at temperatures from 230 to 450 °C and the weight loss in dry N_2 was twice as high as that in humid N_2. Weigh loss from 230 to 450 °C in dry and humid N_2 was 23.0% and 10.7–11.0%, respectively, while the weight loss in stagnant air was 14.9%. In addition, the temperatures at which weight loss was completed were decreased with increasing H_2O partial pressure. The entire decomposition of stoichiometric ZHC (1 mol) into ZnO (5 mol) theoretically leads to a weight loss of 26.27%. However, the total weight loss observed in dry N_2 and stagnant air was 37.5% and 29.7%, respectively. The weight loss observed in the both atmospheres is considerably higher than the theoretical value. In contrast, the total weight loss observed in humid N_2 was 26.3%, in good agreement with the theoretical value.

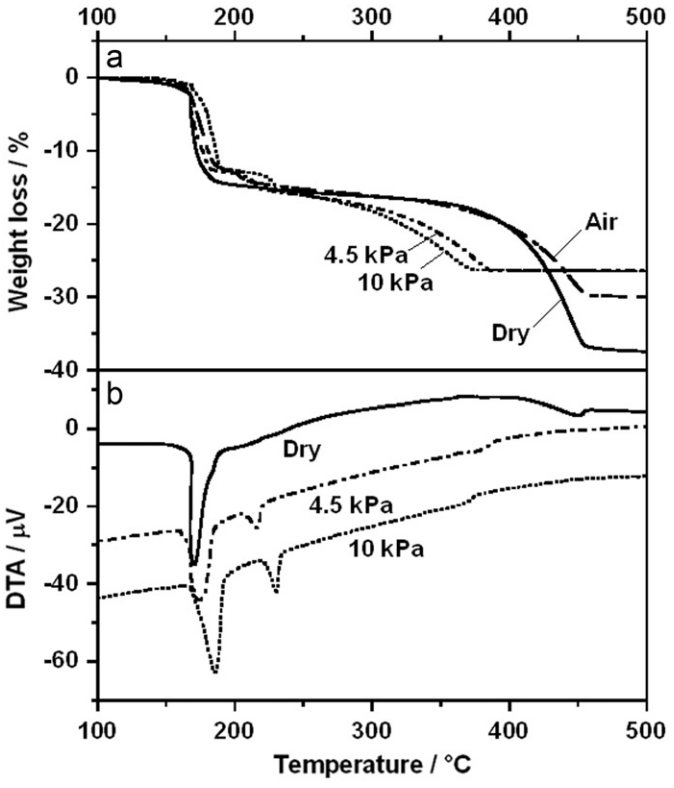

Fig. 3. (a) TG and (b) DTA curves of ZHC in dry N_2, stagnant air, and humid N_2 with P_{H_2O}=4.5 and 10 kPa.

3.3. Thermal decomposition of ZHC

The results shown in Fig. 3 clearly indicated that the total reaction to yield ZnO in humid N_2 was completed at lower temperatures than that in stagnant air and dry N_2. Therefore, it is expected that ZnO can be prepared at low temperatures when thermal decomposition of ZHC is carried out in water vapor. Consequently the thermal decomposition of ZHC was conducted in stagnant air and 100% water vapor by a tubular furnace equipped with a water evaporator. Fig. 4 shows the XRD patterns of the products obtained by the calcinations of ZHC at 300–500 °C for 30 min in stagnant air and water vapor. The XRD patterns were recorded at room temperature and the products were spread on a nonreflecting sample holder without grinding. After calcinations of ZHC at 300 and 350 °C for 30 min in stagnant air, the XRD results showed that the products consisted of the ZHC (unmarked peaks), β-Zn(OH)Cl, and ZnO phases. As discussed later, the ZHC phase is low crystalline because it is reproduced from the thermally decomposed products during the cooling process to room temperature. By calcination at 400 °C for 30 min, the ZHC and β-Zn(OH)Cl phases were disappeared and ZnO was the single-phase in the products. The (002) peak intensity of ZnO was extremely high, which indicated the highly *c*-axis oriented structure in ZnO particles. This result obtained in stagnant air is consistent with the previous report [18]. In contrast, the ZnO single-phase was obtained by calcination of ZHC at 350 °C for 30 min in water vapor. The formation of ZnO in water vapor was 50 °C lower than that in stagnant air. However, it was found that the ZnO formed in water vapor did not show a preferred orientation. Water vapor is considered to influence the crystal growth of ZnO.

Fig. 5 shows the SEM images of ZnO sheets obtained by calcinations in stagnant air and water vapor. The SEM images show that the ZnO particles obtained in the both atmospheres completely

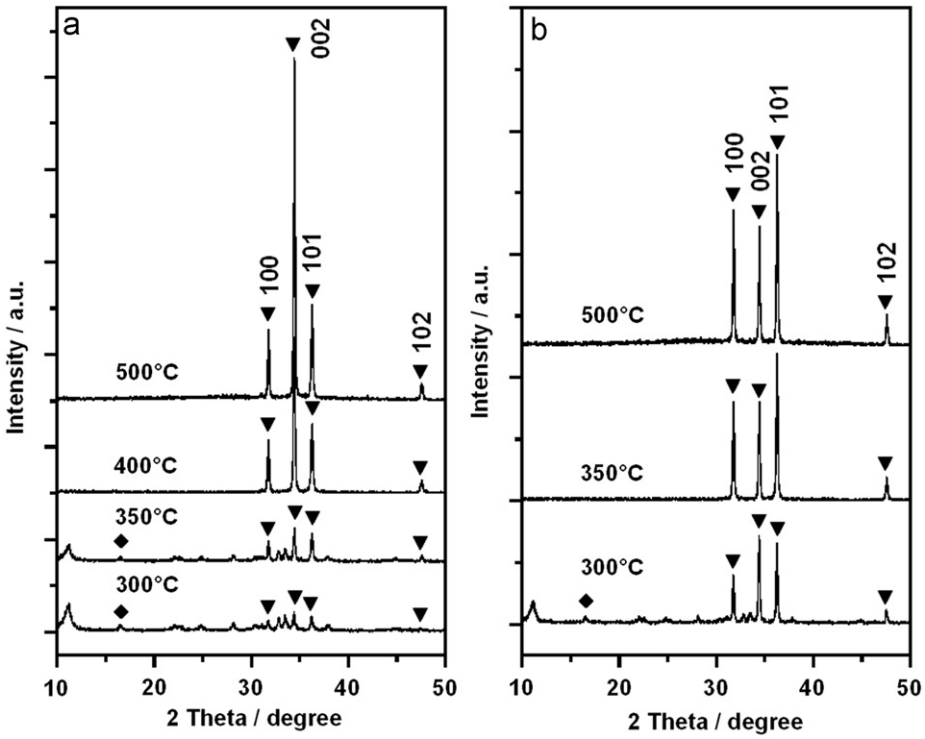

Fig. 4. XRD patterns of the samples obtained by calcinations of ZHC for 30 min in (a) stagnant air and (b) 100% water vapor: (▼) ZnO with labeled *hkl* and (◆) β-Zn(OH)Cl. The unmarked peaks are identified to be ZHC.

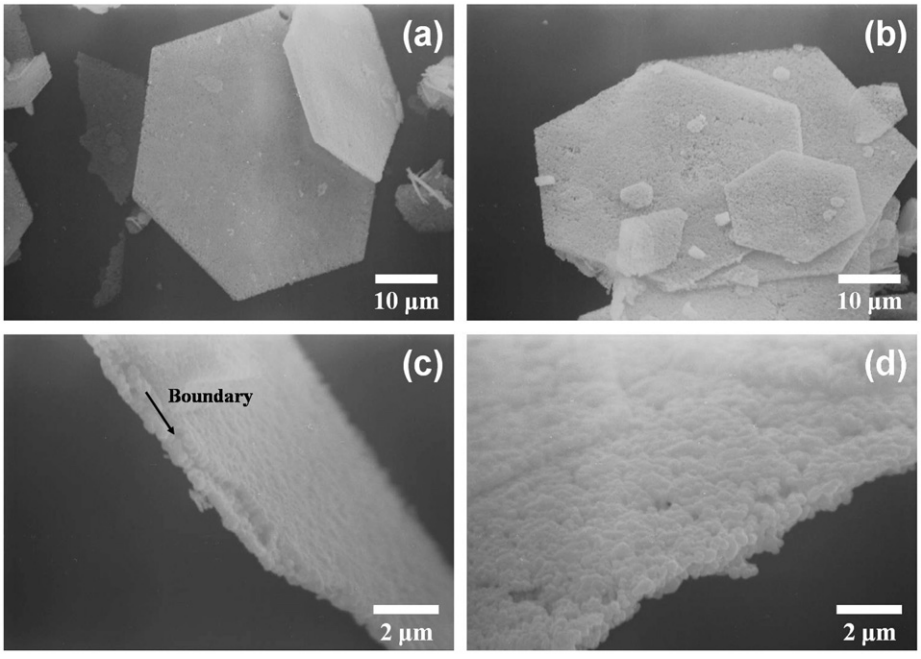

Fig. 5. SEM images of ZnO sheets obtained by calcinations of ZHC for 30 min at (a, c) 400 °C in stagnant air and at (b, d) 350 °C in 100% water vapor: (a, b) overall image and (c, d) fracture surface of ZnO sheet.

maintain the hexagonal morphology of the original ZHC crystals (Fig. 5a and b). The cross section of ZnO sheet obtained in stagnant air shows that the dense and flat ZnO sheet consists of column-like particle arrays with a boundary observed in the center of the cross section of the thin ZnO sheet (Fig. 5c), as observed previously [18]. However, the ZnO sheet obtained in water vapor (Fig. 5d) did not have the boundary and consisted of relatively large ZnO particles with an average size about 0.4 μm.

4. Discussion

4.1. The role of $ZnCl_2$ in the thermal decomposition of ZHC

The results of the XRD–DSC measurements shown in Fig. 2 revealed that the ZnO single-phase was obtained at high temperatures beyond 230 °C through the intermediate compound, β-Zn(OH)Cl. On the other hand, TG-DTA results shown in Fig. 3

indicated that the additional weight loss was occurred at higher temperatures after the formation of the ZnO single-phase. Garcia-Martinez et al. [20] indicated the presence of residual amorphous $ZnCl_2$ in the formed ZnO. To clarify the role of residual $ZnCl_2$, reversed thermal analysis of the ZHC was conducted by heating pattern (B) (see Section 2).

Fig. 6 shows the entire XRD–DSC plots obtained by heating pattern (B) in humid N_2 with $P_{H_2O}=10$ kPa. In the first heating process up to 230 °C, ZHC was decomposed to ZnO (red XRD pattern) through the intermediate compound. When the sample was cooled down to 55 °C after keeping at 230 °C for 10 min, DSC curve showed the two exothermic peaks. The corresponding XRD patterns indicated that the first sharp exothermic peak ($T_{max}=208.3$ °C) and second broad exothermic peak between 65 and 55 °C ($T_{max}=59.6$ °C) corresponds to the regeneration of β-Zn(OH)Cl (green XRD pattern) and ZHC (blue XRD pattern), respectively. The regeneration of β-Zn(OH)Cl suggests the residual presence of $ZnCl_2$ in the formed ZnO and its regeneration mechanism has been proposed by Garcia-Martinez et al. [20]:

$$ZnCl_2+ZnO+H_2O \rightarrow 2\beta\text{-}Zn(OH)Cl \quad (1)$$

The XRD patterns recorded at 55 °C (time scale: 100–300 min) indicated that the reproduced β-Zn(OH)Cl was disappeared when the ZHC began to be formed, and ZnO was consumed by the regeneration of ZHC. Thus, the regeneration process of ZHC can be expressed by following reaction:

$$2\beta\text{-}Zn(OH)Cl+3ZnO+4H_2O \rightarrow Zn_5(OH)_8Cl_2\cdot H_2O \quad (2)$$

The regeneration process of ZHC occurs through the regeneration of β-Zn(OH)Cl in the cooling process. The *c*-axis orientation of β-Zn(OH)Cl and ZHC was lost by the regeneration reactions in the cooling process. In the reheating process in humid N_2, the reproduced ZHC was decomposed to ZnO and β-Zn(OH)Cl at 174.0 °C and the continuous decomposition of β-Zn(OH)Cl occurred at 235.1 °C.

In contrast, the cooling process in dry N_2 showed only the regeneration of β-Zn(OH)Cl. In dry N_2, the amount of H_2O in the atmosphere must be very small. Therefore, it is considered that H_2O required for the regeneration of β-Zn(OH)Cl would be remained in the decomposed products at 230 °C. Thus, the $ZnCl_2$ is considered to remain in the ZnO in the form of hydrated $ZnCl_2$. In the dry atmosphere, H_2O remained together with $ZnCl_2$ in the decomposed products plays a key role in the regeneration of β-Zn(OH)Cl. In contrast, in humid N_2, H_2O in the atmosphere was substantially involved in the regeneration reaction, so that regeneration of β-Zn(OH)Cl and ZHC was promoted.

As mentioned above, the reversed thermal analysis of the ZHC revealed the presence of amorphous $ZnCl_2$ in the decomposed products at 230 °C. In fact, ZHC and β-Zn(OH)Cl formed by the regeneration reaction were detected in the samples calcined at low temperatures in a tubular furnace (Fig. 4).

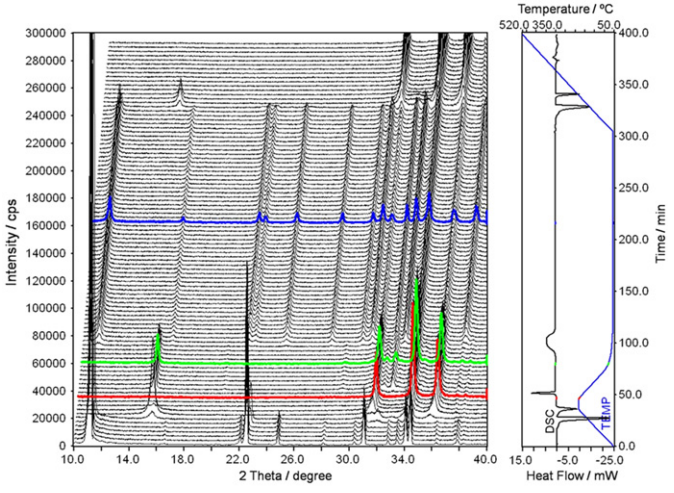

Fig. 6. XRD–DSC plots obtained by heating pattern (B) of ZHC in humid N_2 with $P_{H_2O}=10$ kPa (for interpretation of the references to color in this figure, the reader is referred to the web version of this article).

4.2. Decomposition mechanism of the ZHC

The results indicated above suggest that the ZHC is thermally decomposed to ZnO through β-Zn(OH)Cl as the intermediate phase, leaving amorphous hydrated $ZnCl_2$ in dry and humid N_2. Garcia-Martinez et al. [20] have proposed the decomposition mechanism of ZHC in terms of a heating rate. When the thermal decomposition of ZHC was conducted at a high heating rate (10 °C/min), the smaller amount of H_2O remained together with $ZnCl_2$ in the decomposed products than that in the case of a low heating rate (1 °C/min). Consequently, the decomposition of residual $ZnCl_2$ at a high heating rate resulted in the partial hydrolysis and vaporization of $ZnCl_2$ [20]. In this paper, we propose the decomposition mechanism of ZHC in terms of an atmospheric humidity. The decomposition mechanism of ZHC in dry and humid N_2 can be proposed as shown in Fig. 7. Square bracket indicates the proposed intermediate compound.

As shown in Fig. 3, up to 230 °C, ZHC is decomposed by two step dehydration reactions in humid N_2. In the first dehydration reaction, the amount of weight loss is 12.7–13.0% and this weight loss corresponds to the release 4 mol of H_2O. Thus, 1 mol of ZHC is decomposed to 2 mol of β-Zn(OH)Cl and 3 mol of ZnO releasing 4 mol of H_2O (expected weight loss: 13.06%). By the second dehydration reaction, the weight loss of 2.5–2.8% was observed. This result suggests that 0.75 mol of H_2O is released from 2 mol of β-Zn(OH)Cl (expected weight loss: 2.45%) and the trace amounts of H_2O (0.25 mol) remains with amorphous $ZnCl_2$ in the formed ZnO. The remained water may exist in the form of hydrated $ZnCl_2$. The amounts of weight loss in dry and humid N_2 up to 230 °C are 14.5% and 15.5%, respectively. The weight loss in dry N_2 up to 230 °C is very close to that in humid N_2 though two dehydration reactions are overlapped. It is concluded that the decomposition process of ZHC by heating up to 230 °C is same in the both atmospheres. In addition, mass spectral analysis of the evolved gaseous products was conducted in flowing He in order to confirm the proposed mechanism. Only the signal for mass 18, corresponding to H_2O, was detected up to 230 °C. This result shows that any compounds including chlorine are not released by heating to 230 °C.

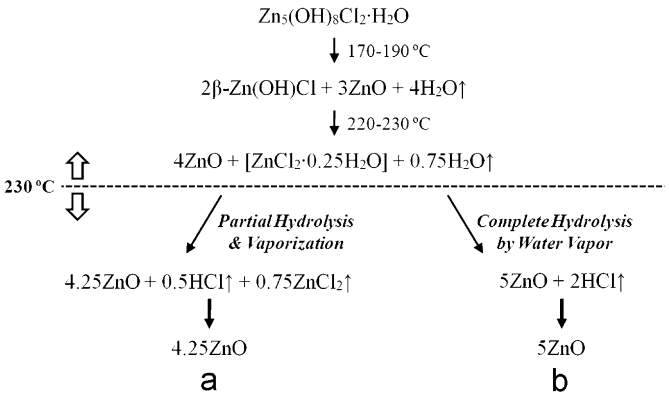

Fig. 7. Proposed reaction steps during the decomposition of $Zn_5(OH)_8Cl_2\cdot H_2O$ in (a) dry N_2 and (b) humid N_2.

Above 230 °C, the decomposition behavior of residual hydrated $ZnCl_2$ is different depending on the atmospheric humidity. When the residual $ZnCl_2$ is partially hydrolyzed by the remained water and 0.75 mol of $ZnCl_2$ vaporizes, the weight loss is calculated to be 21.82%. The weight loss in dry N_2 above 230 °C is 23.0%, which is close to the expected value. Thus, the entire decomposition of stoichiometric ZHC in dry N_2 gives 4.25 mol of ZnO, as shown in Fig. 7a. However, the weight loss in humid N_2 above 230 °C is 10.7–11.0%. In humid N_2 (Fig. 7b), the hydrolysis of the residual $ZnCl_2$ is assisted by the presence of excess H_2O in the atmosphere. Since the weight loss in humid N_2 up to 230 °C is 15.5%, the observed total weight loss in humid N_2 shows good agreement with theoretical value (26.27%) to yield 5 mol of ZnO from 1 mol of ZHC. Therefore, it can be concluded that in humid N_2, ZHC is theoretically decomposed to ZnO without vaporization of $ZnCl_2$.

It is noteworthy that in stagnant air, the residual $ZnCl_2$ is partially hydrolyzed and vaporizes because of a small amount of H_2O in the atmosphere. The total weight loss in stagnant air (29.7%) corresponds to the formation of 4.77 mol of ZnO.

Hydrolysis of the residual $ZnCl_2$ is especially sensitive to the humidity of heating atmosphere. According to the TG curves (Fig. 3), weight loss was completed at 451 °C in dry N_2, and at 387 and 373 °C in humid N_2 with $P_{H_2O}=4.5$ and 10 kPa, respectively. These points show the temperatures at which the residual $ZnCl_2$ is completely converted to ZnO. Unfortunately no signals for chloride compounds such as HCl and $ZnCl_2$ were detected by the mass spectral analysis of the gas produced by the thermal decomposition of ZHC. These compounds were formed at high temperatures beyond 230 °C and might be condensed before the detector. However, the proposed mechanism for the thermal decomposition of ZHC in this study is reasonable from the results of XRD–DSC and TG-DTA measurements.

4.3. Crystal growth of the ZnO

XRD results in humid N_2 (Fig. 2) showed that the intermediate β-Zn(OH)Cl phase formed by the decomposition of ZHC has highly *c*-axis oriented structure as well as ZnO. The *c*-axis orientation of the reaction products is ascribed to the layered structure of ZHC [25].

After calcinations in stagnant air and 100% water vapor in the tubular furnace, the obtained ZnO particles maintained the hexagonal morphology (Fig. 5) of the original ZHC crystals but their (002) orientation observed in the XRD patterns were different, depending on the humidity of the atmosphere (Fig. 4). According to the SEM image of fractured ZnO sheet (Fig. 5c), the growth mechanism of the ZnO in stagnant air is considered as follows. The nucleation of ZnO starts on the surface of the ZHC sheets, and these nuclei grow inside during the heating process to form the column-like particles. Finally the column-like particles meet with each other in the middle of the sheets to form the boundary [19]. Thus, the highly *c*-axis oriented ZnO sheets are obtained in stagnant air. A similar growth mechanism is known in the formation of MgO by the thermal decomposition of hexagonal $Mg(OH)_2$ [26,27]. Anderson and Horlock [26] have reported that the decomposition reaction proceeds along the *c*-axis from the outer edge of hexagonal plate-like $Mg(OH)_2$ and the water molecule is released parallel to the (0001) plane. In contrast, in 100% water vapor, the *c*-axis oriented structure in ZnO particles is not observed. The ZnO nuclei would be formed randomly in the ZHC sheets due to the accelerated nucleation by water. In the water vapor atmosphere, the decomposition reaction would proceed from inside because water is able to enter between layers of the ZHC crystal.

Fig. 8 shows the integrated XRD peak intensities of ZnO (002), (101), and (100) diffraction in dry N_2 and humid N_2 with $P_{H_2O}=4.5$ kPa obtained from XRD–DSC measurements as shown in Fig. 2. When ZnO was first formed in dry N_2, the intensity of the

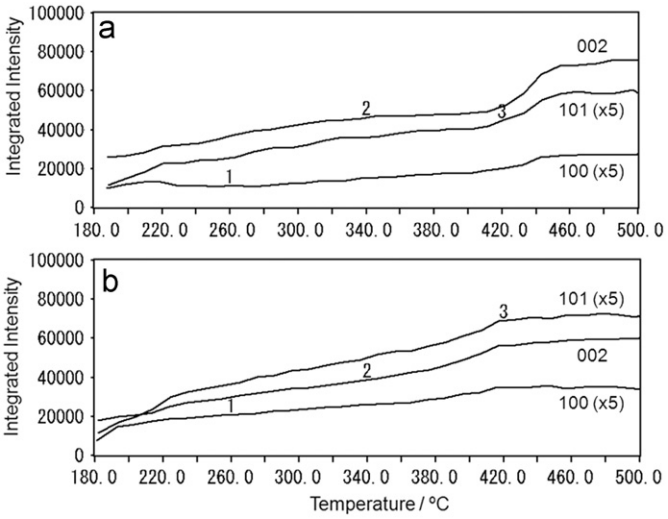

Fig. 8. Integrated XRD peak intensities of the ZnO in (a) dry N_2 and (b) humid N_2 with $P_{H_2O}=4.5$ kPa obtained from XRD–DSC measurements as shown in Fig. 2. Curve 1: (100) peak at 30.8–32.2°, curve 2: (002) peak at 33.5–35.2°, and curve 3: (101) peak at 35.3–37.0°.

(002) peak was higher than that of (101) and (100) peaks. In dry N_2, the *c*-axis oriented ZnO was initially formed. Integrated intensities of these three peaks were gradually increased up to 420 °C and then rapidly increased between 420 and 460 °C because of the formation of ZnO by the hydrolysis of the residual $ZnCl_2$ and elimination of the gas products. It is well-known that ZnO usually has the *c*-axis oriented growth habits via gas-phase deposition [28–30]. In contrast, the intensity of each diffraction peak of ZnO is comparable in the initial stage of the formation of ZnO in humid N_2. The intensity of the (002) peak was lower and that of the (101) peak was higher than that observed in dry N_2. Thus, the ZnO nuclei were formed without preferred orientation in humid N_2. Integrated intensities of (101), (002), and (100) peaks were securely increased up to 420 °C in humid N_2 with increasing temperature. Thus, the ZnO crystals generated at lower temperature in humid N_2 and grew larger in all directions.

5. Conclusions

Thermal decomposition process of ZHC prepared by hydrothermal slow-cooling method has been investigated by using XRD–DSC and TG-DTA in a humidity-controlled atmosphere to clarify the effect of water vapor. ZHC was decomposed to ZnO through β-Zn(OH)Cl as the intermediate phase, leaving amorphous hydrated $ZnCl_2$. In dry N_2, significant weight loss was caused by the vaporization of residual $ZnCl_2$. On the other hand, in humid N_2, the hydrolysis of $ZnCl_2$ was accelerated and the formation of ZnO was completed at low temperature. The observed total weight loss in humid N_2 showed good agreement with the theoretical value.

Calcinations in stagnant air, ZnO single-phase remained with the morphology from ZHC crystals was obtained at 400 °C for 30 min and consisted of *c*-axis oriented column-like particle arrays. Although ZnO single-phase was obtained at 350 °C for 30 min in 100% water vapor, the *c*-axis orientation of ZnO was collapsed. The ZnO nuclei would be formed randomly in the ZHC sample by water vapor.

References

[1] S.P. Newman, W. Jones, J. Sold, State Chem. 148 (1999) 26–40.
[2] S. Aisawa, H. Kudo, T. Hoshi, S. Takahashi, H. Hirahara, Y. Umetsu, E. Narita, J. Sold, State Chem. 177 (2004) 3987–3994.

[3] R. Ma, Z. Liu, K. Takada, N. Iyi, Y. Bando, T. Sasaki, J. Am. Chem. Soc. 129 (2007) 5257–5263.
[4] C.G. Silva, Y. Bouizi, V. Fornés, H. Carcía, J. Am. Chem. Soc. 131 (2009) 13833–13839.
[5] M.D. Arco, S. Gutiérrez, C. Martín, V. Rives, J. Rocha, J. Solid State Chem. 177 (2004) 3954–3962.
[6] G.G.C. Arizaga, K.G. Satyanarayana, F. Wypych, Solid State Ionics 178 (2007) 1143–1162.
[7] E.D. Rodeghiero, J. Chisaki, E.P. Giannelis, Chem. Mater. 9 (1997) 478–484.
[8] E. Hosono, S. Fujihara, I. Honma, H. Zhou, J. Mater. Chem. 15 (2005) 1938–1945.
[9] K. Petrov, A. Lyubchova, L. Markov, Polyhedron 8 (1989) 1061–1067.
[10] S.M. Haile, D.W. Johnson, G.H. Wiseman, H.K. Bowen, J. Am. Ceram. Soc. 72 (1989) 2004–2008.
[11] Q. Zhang, C.S. Dandeneau, X. Zhou, G. Cao, Adv. Mater. 21 (2009) 4087–4108.
[12] Z.L. Wang, J. Song, Science 312 (2006) 242–246.
[13] H. Morioka, H. Tagaya, J.I. Kadokawa, K. Chiba, J. Mater. Sci. Lett. 18 (1999) 995–998.
[14] E. Hosono, S. Fujihara, T. Kimura, H. Imai, J. Colloid Interface Sci. 272 (2004) 391–398.
[15] T. Biswick, W. Jones, A. Pacula, E. Serwicka, J. Podobinski, Solid State Sci. 11 (2009) 330–335.
[16] T. Biswick, W. Jones, A. Pacula, E. Serwicka, J. Podobinski, J. Solid State Chem. 180 (2007) 1171–1179.
[17] N. Audebrand, J.P. Auffrédic, D. Louër, Chem. Mater. 10 (1998) 2450–2461.
[18] W. Zhang, K. Yanagisawa, Chem. Mater. 19 (2007) 2329–2334.
[19] T. Arii, A. Kishi, Thermochim. Acta 400 (2003) 175–185.
[20] O. Garcia-Martinez, E. Vila, J.L. Martin de Vidales, R.M. Rojas, K.J. Petrov, J. Mater. Sci. 29 (1994) 5429–5434.
[21] O.K. Srivastava, E.A. Secco, Can. J. Chem. 45 (1967) 579–583.
[22] I. Rasines, J.I. Morales de Setién, Thermochim. Acta 37 (1980) 239–246.
[23] G.M. Lombardo, G.C. Pappalardo, F. Constantino, U. Constantino, M. Sisani, Chem. Mater. 20 (2008) 5585–5592.
[24] H. Zhang, S.H. Guo, K. Zou, X. Duan, Mater. Res. Bull. 44 (2009) 1062–1069.
[25] F.C. Hawthorne, E. Sokolova, Can. Miner. 40 (2002) 939–946.
[26] P.J. Anderson, R.H. Horlock, Trans. Faraday Soc. 58 (1962) 1993–2004.
[27] J. Green, J. Mater. Sci. 18 (1983) 637–651.
[28] Y. Zhang, F. Lu, Z. Wang, L. Zhang, J. Phys. Chem. C 111 (2007) 4519–4523.
[29] C. Li, G. Fang, J. Li, L. Ai, B. Dong, X. Zhao, J. Phys. Chem. C 112 (2008) 990–995.
[30] A. Umar, C. Ribeiro, A. Al-Hajry, Y. Masuda, Y.B. Hahn, J. Phys. Chem. C 113 (2009) 14715–14720.